Title:

Expression dynamics of ARGONAUTE proteins during meiosis in Arabidopsis

Authors and affiliation:

Cecilia Oliver and German Martinez.

Department of Plant Biology, Uppsala BioCenter, Swedish University of Agricultural Sciences and Linnean Center for Plant Biology, Uppsala, Sweden

Corresponding authors:

Cecilia Oliver: cecilia.oliver.velasco@slu.se

German Martinez: german.martinez.arias@slu.se

ORCID information:

Cecilia Oliver: 0000-0002-5231-7910

German Martinez: 0000-0002-5215-0866

Abstract

Meiosis is a specialized cell division that is key for reproduction and genetic diversity in sexually reproducing plants. Recently, different RNA silencing pathways have been proposed to carry a specific activity during meiosis, but the pathways involved during this process remain unclear. Here, we explored the subcellular localization of different ARGONAUTE (AGO) proteins, the main effectors of RNA silencing, during male meiosis in *Arabidopsis thaliana* using immunolocalizations with commercially available antibodies. We detected the presence of AGO proteins associated with posttranscriptional gene silencing (AGO1, 2 and 5) in the cytoplasm or the nucleus, while AGOs associated with transcriptional gene silencing (AGO4 and 9) localized exclusively in the nucleus. These results indicate that the localization of different AGOs correlates with their predicted roles at the transcriptional and posttranscriptional levels and provide an overview of their timing and potential role during meiosis.

Introduction

Meiosis is a special type of cell division where one round of DNA synthesis is followed by two rounds of cell division, segregating homologous chromosomes during the first division and sister chromatids at the second division (Marston et al. 2004, Mercier et al. 2015). This process is key for the production of gametes and the reshuffling of the genetic information during sexual reproduction (Bolcun-Filas et al. 2018). The mechanisms regulating meiosis have been widely studied at the cellular, genetic, and molecular levels in a variety of organisms. In plants, more than 90 genes have been identified comprising

38 different meiotic processes that include double-strand break (DSB) formation,
39 chromosome segregation or meiotic recombination (Huang et al. 2019a). Intriguingly, in
40 the recent years it has been revealed that several of these processes involve the RNA
41 silencing machinery (Oliver et al. 2016, Underwood et al. 2018, Wei et al. 2012). Different
42 RNA silencing pathways are active during meiosis (Huang et al. 2020, Huang, et al.
43 2019a, Yelina et al. 2015). The miRNA affects chromatin condensation and the number
44 of chiasmas, while the RNA-directed DNA methylation (RdDM) pathways affects
45 chromatin condensation, the number of chiasmas and chromosome segregation (Oliver
46 et al. 2017, Oliver, et al. 2016). Moreover, the RdDM pathway protects euchromatic
47 regions from meiotic recombination (Yelina, et al. 2015). Additionally, *Arabidopsis* a non-
48 canonical RNA silencing pathway plays a role in double-strand break repair (Wei, et al.
49 2012). Moreover, meiocyte-specific sRNAs between 23-24 nts are positively correlated
50 with genes that have a meiocyte-preferential expression pattern (Huang, et al. 2019a),
51 which could correlate with the observed role of DNA methylation in the regulation of gene
52 expression in meiocytes (Walker et al. 2018). ARGONAUTE (AGO) proteins are the
53 effectors of the different RNA silencing pathways and have dedicated members that act
54 at the posttranscriptional or transcriptional levels. Here, we analyze the subcellular
55 localization of the main AGO proteins in Arabidopsis during the different meiosis stages,
56 which provides a confirmation of their activity during this process.

57

58 **Materials and Methods**

59

60 **Plant material**

Plants used for immunolocalization analysis were grown in a phytotron under long day conditions (16-hour light/8-hour dark photoperiod), at 24-25 °C and 45% relative humidity.

Bioinformatic analysis

sRNA data was downloaded from the SRA repository project number PRJNA510650 (Huang et al. 2019b). sRNA alignments were performed using bowtie (Langmead et al. 2009) with the following parameters –t –v2 that allows 2 mismatches to the alignments. For sRNA categorization a miRNAs, sRNA libraries were aligned to individual indexes generated for each genomic category and compared total sRNAs mapping to the TAIR10 chromosome sequences. Transcriptomic data corresponds to the ATH1 data from GSE10229 and GSE13000 (Libeau et al. 2011) and data extracted using the CATdb database (http://urgv.evry.inra.fr/cgi-bin/projects/CATdb/catdb_index.pl).

Cytology:

Immunolocalization on meiotic nuclei were carried out by squash technique as was previously described by Manzanero et al. (2000) with some modifications (Oliver et al., 2013). Two bioreplicates of young buds from five plants each, were analyzed. The primary antibodies used were rabbit anti-AGO1 (1:200 AS09 527), -AGO2 (1:100, AS13 2682), -AGO5 (1:100, AS10 671), -AGO4 (1:100, AS09 617), -AGO6 (1:50, AS10 672), -AGO9 (1:100, AS10 673) and -AGO10 (1:50, AS15 3071) antibodies from Agrisera. Secondary antibody used was goat anti-rabbit IgG H&L Alexa Fluor 568 conjugated (1:200; ab175471; Abcam). The slides were stained with the DAPI, 1 µg/ml during 20-30 min and finally mounting with antifading medium (0.2% n-propyl Gallete, 0.1% DMSO, 90% glycerol in PBS). Fluorescent signals were observed using an epifluerescence microscope Zeiss Axio Scope A1. Images were captured with AxioCam ICc5 camera and were analyzed and processed with ImageJ and Affinity Photo software.

Results

89 To discern the level of expression of RNA silencing components in meiocytes, we
90 analyzed their expression from publicly available microarray datasets (Libeau, et al. 2011)
91 (Figure 1 and Supplementary Methods). Overall, several components from the RNA
92 silencing pathways were preferentially expressed in meiocytes compared to somatic
93 tissues (Figure 1A), including the AGO proteins AGO4, 5 and 10, the Dicer-like (DCL)
94 proteins DCL1, 3 and 4 or the sRNA methyltransferase HEN1. This indicated that different
95 PTGS (AGO5, DCL1 and DCL4) and TGS (AGO4 and DCL3) pathways might be
96 especially active during meiosis. Previous analysis (Huang, et al. 2019a) have shown that
97 TE-derived sRNAs accumulate to relatively high levels in meiocytes and that certain
98 miRNAs like miR845 are active before the microspore stage (Borges et al. 2018).
99 Although miRNAs were not globally enriched in meiocytes (Figure 1B), several miRNAs
100 were strongly upregulated including miR839, miR780.2, miR780.1, miR157, miR172,
101 miR166 and miR860, which are important regulators of several transcription factor
102 families (Figure 1C, Supplementary Figure 1 and Supplementary Table 2). In summary,
103 transcriptomic and sRNA sequencing analysis supported the notion that the RNA
104 silencing machinery might have a meiocyte-specific activity.

105

106 Although transcriptomic analysis is important to infer the activity of the different RNA
107 silencing pathways in meiocytes, this analysis provides a steady image of this tissue and
108 ignores, for example, its dynamism during meiosis. To understand the subcellular
109 localization and dynamics of the different AGO proteins during meiosis, we performed
110 immunolocalizations of the AGO proteins that had commercially available antibodies
111 (Agrisera, AGO1, 2, 4, 5, 6, 9 and 10, Figure 2 and Supplementary Methods). During

112 meiosis all AGOs but AGO6 and AGO10 could be detected. In detail, AGO1 and its
113 paralogs AGO2 and AGO5 displayed a similar localization and expression pattern during
114 the first meiotic stages (Figure 2A, 2B, 2C). The three proteins were located mainly in the
115 cytoplasm, similar to their localization in somatic tissues (Bologna et al. 2018, Ye et al.
116 2012). From the leptotene to the diplotene stage these three AGO proteins formed
117 cytoplasmic granules (Figure. 2A1, 2B1, 2C1). In somatic tissues, cytoplasmic bodies are
118 involved in the degradation and translation arrest of mRNAs (Maldonado-Bonilla 2014).
119 In mammals, AGO proteins localize in P-bodies where they mediate the translational
120 repression of their target mRNAs (Liu et al. 2005). The localization pattern observed for
121 AGO1, 2 and 5 might indicate a similar role of RNA silencing in the posttranscriptional
122 regulation of mRNAs, a process that is known to take place in other organisms like
123 mammals (Yao et al. 2015).

124

125 Despite the similarities between the accumulation during meiosis, AGO1, 2 and 5, they
126 showed differences in their dynamics during meiosis. For example, AGO1 condensates
127 around the nuclear envelope at diplotene (Figure 2A4) but after this stage, it showed a
128 disperse accumulation (Figure 2A5). This location during cell division could be related
129 with the known AGO1 association with the endoplasmic reticulum (Li et al. 2013), as when
130 the nuclear envelope disassembles it reorganizes in vacuoles around the bivalents
131 (Marston, et al. 2004, Mercier, et al. 2015). AGO5 displayed a similar pattern of
132 subcellular localization to AGO1, although its localization at cytoplasmic bodies
133 disappeared at diplotene (Figure 2B4). On the other hand, AGO2 showed a dual
134 localization in the cytoplasm and in the nucleus (Figure 2C1-4) and was not detectable

135 after metaphase I (Figure 2C5-6). Both its nucleocytoplasmic localization and timing of
136 expression are in line with its known role in double strand break (DSB) repair, which takes
137 place during the first meiotic stages (Oliver et al. 2014, Wei, et al. 2012). Nevertheless,
138 AGO2 expression pattern was recapitulated after the second meiotic division (Figure
139 2C7), indicating that it might serve other roles in parallel to its function in DSB repair
140 during meiosis.

141

142 On the other hand, the TGS/RdDM-associated AGO proteins, AGO4 and AGO9, were
143 located in the nuclei during all meiotic stages (Figure 2D and E). Exceptionally, at
144 metaphase I, when the nuclear envelope dissolves, both proteins showed a dispersed
145 accumulation. This is in accordance with the known role of the RdDM pathway in
146 regulating DNA methylation during meiosis (Walker, et al. 2018). Meiocytes have the
147 lowest CHH methylation values of all the reproductive nuclei analyzed, but its activity is
148 needed for the regulation of gene expression (Walker, et al. 2018). We detected a low
149 accumulation of AGO4 and 9 after metaphase I (Figure 2D5-6 and 2E5-6), which might
150 partially cause this reduction in CHH methylation. Interestingly, we observed that AGO9
151 displayed a localization pattern compatible with a preference for heterochromatic regions
152 at pachytene. This localization might explain the known role of AGO9 on the dissolution
153 of interlocks during meiosis (Oliver, et al. 2014).

154

155 **Discussion**

156 In summary, our results provide an overview of the subcellular localization, timing and
157 potential role of different RNA silencing pathways during meiosis. Furthermore, our work
158 complements previous analysis that analyzed RNA silencing activity in meiocytes, and
159 opens the door for future molecular analysis of the specific role of AGO proteins during
160 specific meiosis stages, which are technically challenging at the moment.

161

162 **Author contribution statement:** C.O and G.M. design the experiments and wrote the
163 manuscript. C.O. performed the experiments and analyzed the data. G.M. analyzed the
164 bioinformatic data.

165

166 **Acknowledgements**

167 The authors thank SLU, the Carl Tryggers Foundation (CTS 17-305 and CTS 18-251),
168 the Swedish Research Council (VR 2016-05410) and the Knut and Alice Wallenberg
169 Foundation (KAW 2019-0062) for supporting research in the Martinez group. The data
170 handling was enabled by resources provided by the Swedish National Infrastructure for
171 Computing (SNIC) at UPPMAX partially funded by the Swedish Research Council through
172 grant agreement no. 2018-05973.

173

174 **References:**

175 Bolcun-Filas E, Handel MA (2018) Meiosis: the chromosomal foundation of reproduction.
176 Biol Reprod 99:112-126

177 Bologna NG, Iselin R, Abriata LA, Sarazin A, Pumplin N, Jay F, Grentzinger T, Dal Peraro
178 M, Voinnet O (2018) Nucleo-cytosolic Shuttling of ARGONAUTE1 Prompts a
179 Revised Model of the Plant MicroRNA Pathway. Mol Cell 69:709-719 e705
180 Borges F, Parent JS, van Ex F, Wolff P, Martinez G, Kohler C, Martienssen RA (2018)
181 Transposon-derived small RNAs triggered by miR845 mediate genome dosage
182 response in Arabidopsis. Nat Genet 50:186-192
183 Huang J, Wang C, Li X, Fang X, Huang N, Wang Y, Ma H, Wang Y, Copenhaver GP
184 (2020) Conservation and Divergence in the Meiocyte sRNAomes of Arabidopsis,
185 Soybean, and Cucumber. Plant Physiol 182:301-317
186 Huang J, Wang C, Wang H, Lu P, Zheng B, Ma H, Copenhaver GP, Wang Y (2019a)
187 Meiocyte-Specific and AtSPO11-1-Dependent Small RNAs and Their Association
188 with Meiotic Gene Expression and Recombination. Plant Cell 31:444-464
189 Huang JY, Wang C, Wang HF, Lu PL, Zheng BL, Ma H, Copenhaver GP, Wang YX
190 (2019b) Meiocyte-Specific and AtSPO11-1-Dependent Small RNAs and Their
191 Association with Meiotic Gene Expression and Recombination. Plant Cell 31:444-
192 464
193 Langmead B, Trapnell C, Pop M, Salzberg SL (2009) Ultrafast and memory-efficient
194 alignment of short DNA sequences to the human genome. Genome Biol 10:R25
195 Li S, Liu L, Zhuang X, Yu Y, Liu X, Cui X, Ji L, Pan Z, Cao X, Mo B, Zhang F, Raikhel N,
196 Jiang L, Chen X (2013) MicroRNAs inhibit the translation of target mRNAs on the
197 endoplasmic reticulum in Arabidopsis. Cell 153:562-574

198 Libeau P, Durandet M, Granier F, Marquis C, Berthome R, Renou JP, Taconnat-Soubirou
199 L, Horlow C (2011) Gene expression profiling of Arabidopsis meiocytes. Plant Biol
200 (Stuttg) 13:784-793
201 Liu J, Valencia-Sanchez MA, Hannon GJ, Parker R (2005) MicroRNA-dependent
202 localization of targeted mRNAs to mammalian P-bodies. Nat Cell Biol 7:719-723
203 Maldonado-Bonilla LD (2014) Composition and function of P bodies in Arabidopsis
204 thaliana. Front Plant Sci 5:201
205 Marston AL, Amon A (2004) Meiosis: cell-cycle controls shuffle and deal. Nat Rev Mol
206 Cell Biol 5:983-997
207 Mercier R, Mezard C, Jenczewski E, Macaisne N, Grelon M (2015) The molecular biology
208 of meiosis in plants. Annu Rev Plant Biol 66:297-327
209 Oliver C, Pradillo M, Jover-Gil S, Cunado N, Ponce MR, Santos JL (2017) Loss of function
210 of Arabidopsis microRNA-machinery genes impairs fertility, and has effects on
211 homologous recombination and meiotic chromatin dynamics. Sci Rep 7:9280
212 Oliver C, Santos JL, Pradillo M (2014) On the role of some ARGONAUTE proteins in
213 meiosis and DNA repair in Arabidopsis thaliana. Frontiers in Plant Science 5
214 Oliver C, Santos JL, Pradillo M (2016) Accurate Chromosome Segregation at First Meiotic
215 Division Requires AGO4, a Protein Involved in RNA-Dependent DNA Methylation
216 in Arabidopsis thaliana. Genetics 204:543-553
217 Underwood CJ, Choi K, Lambing C, Zhao X, Serra H, Borges F, Simorowski J, Ernst E,
218 Jacob Y, Henderson IR, Martienssen RA (2018) Epigenetic activation of meiotic
219 recombination near Arabidopsis thaliana centromeres via loss of H3K9me2 and
220 non-CG DNA methylation. Genome Res 28:519-531

221 Walker J, Gao H, Zhang J, Aldridge B, Vickers M, Higgins JD, Feng X (2018) Sexual-
222 lineage-specific DNA methylation regulates meiosis in Arabidopsis. Nat Genet
223 50:130-137
224 Wei W, Ba Z, Gao M, Wu Y, Ma Y, Amiard S, White CI, Rendtlew Danielsen JM, Yang
225 YG, Qi Y (2012) A role for small RNAs in DNA double-strand break repair. Cell
226 149:101-112
227 Yao CC, Liu Y, Sun M, Niu MH, Yuan QQ, Hai YA, Guo Y, Chen Z, Hou JM, Liu Y, He ZP
228 (2015) MicroRNAs and DNA methylation as epigenetic regulators of mitosis,
229 meiosis and spermiogenesis. Reproduction 150:R25-R34
230 Ye R, Wang W, Iki T, Liu C, Wu Y, Ishikawa M, Zhou X, Qi Y (2012) Cytoplasmic assembly
231 and selective nuclear import of Arabidopsis Argonaute4/siRNA complexes. Mol
232 Cell 46:859-870
233 Yelina NE, Lambing C, Hardcastle TJ, Zhao X, Santos B, Henderson IR (2015) DNA
234 methylation epigenetically silences crossover hot spots and controls chromosomal
235 domains of meiotic recombination in Arabidopsis. Genes Dev 29:2183-2202

236

237 **Figure legends:**

238 **Figure 1. Analysis of the expression in meiocytes of different RNA silencing and**
239 **epigenetic pathways components and analysis of miRNA accumulation in**
240 **meiocytes. A.** Heat map of the expression values of RNA silencing and epigenetic
241 pathways components in meiocyte microarray experiments. Expression values are
242 represented as the normalized log2 ratio of the comparison meiocyte/control tissue. **B.**
243 Global accumulation of miRNAs in leaves and meiocytes samples from public datasets

244 normalized to reads per million. **C.** Accumulation values of miRNAs enriched in meiocyte
245 sRNA libraries. Enrichment was considered only for miRNAs accumulating more than 2-
246 fold in meiocytes and with a p-value<0.05.

247

248 **Figure 2. Immunolocalization of AGO1 (A), AGO5 (B), AGO2 (C), AGO4 (D) and**
249 **AGO9 (E) at different representative meiotic stages in Arabidopsis meiocytes.**
250 Leptotene (A1, B1, C1, D1, E1); Zygotene (A2, B2, C2, D2, E2); Pachytene (A3, B3, C3,
251 D3, E3); Diplotene (A4, B4, C4, D4, E4); Diakinesis (B5), Metaphase I (A5, C5, D5, E5)
252 Prophase II (A6, B6, D6, E6); Metaphase II (C6); Tetrad (A7, B7, C7, D7, E7).
253 Immunostaining with antibodies is shown in red, counterstaining with DAPI is shown in
254 grey. Bar indicates 10 µm.

255

256 **Supplementary Figure 1.** Predicted and confirmed targets of miRNA families
257 significantly upregulated in meiocytes.

258

259 **Supplementary Table 1.** Raw values of normalized log2-ratio expression values for
260 selected genes in meiocytes microarray data.

261

262 **Supplementary Table 2.** Raw values of miRNA accumulation in meiocytes and leaf
263 sRNA libraries.

Figure 1

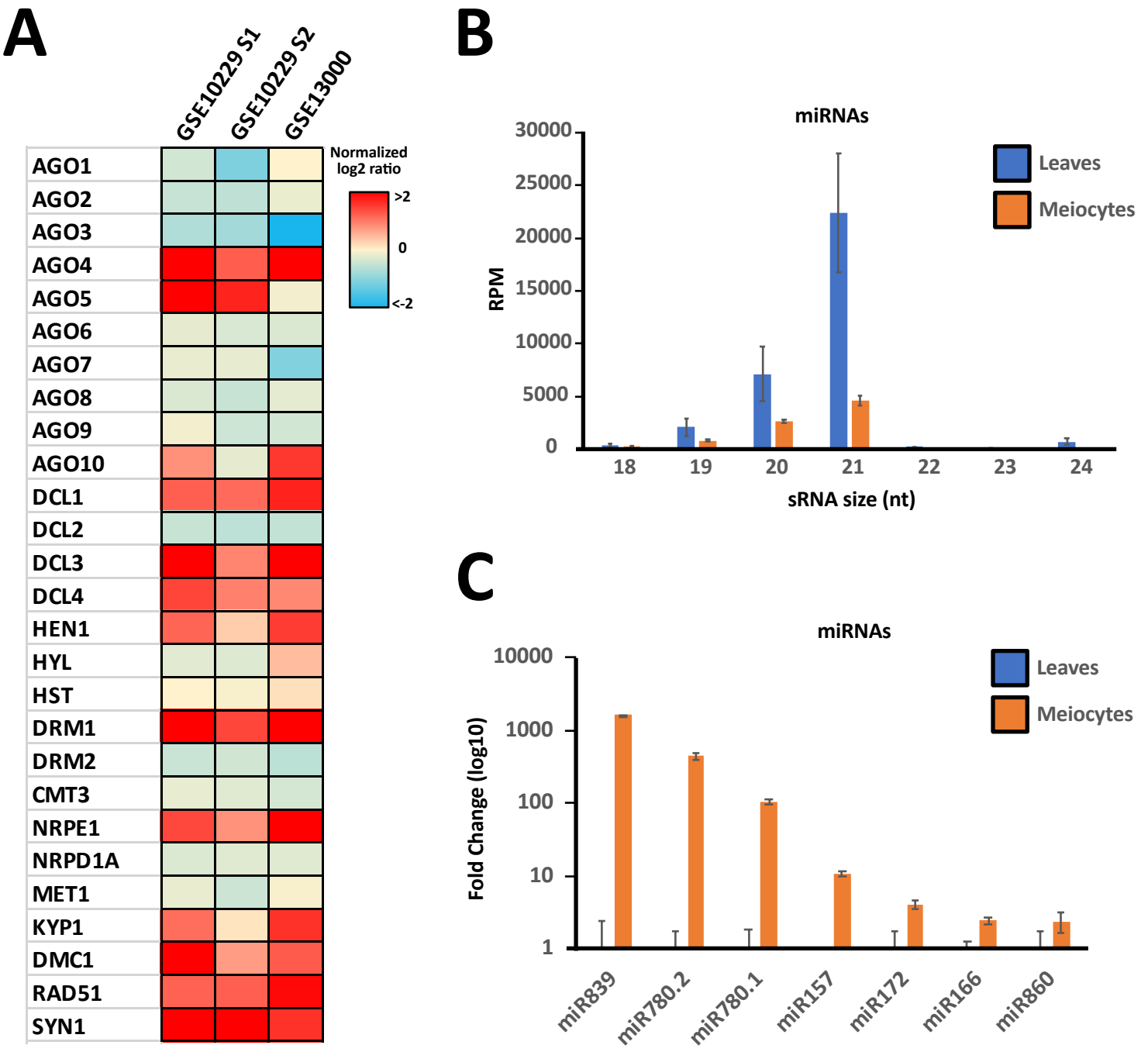
A
GSE10229 S1
GSE10229 S2
GSE13000
Normalized log2 ratio
>2
0
<-2
AGO1
AGO2
AGO3
AGO4
AGO5
AGO6
AGO7
AGO8
AGO9
AGO10
DCL1
DCL2
DCL3
DCL4
HEN1
HYL
HST
DRM1
DRM2
CMT3
NRPE1
NRPD1A
MET1
KYP1
DMC1
RAD51
SYN1
B
miRNAs
RPM
30000
25000
20000
15000
10000
5000
0
18
19
20
21
22
23
24
sRNA size (nt)
Leaves
Meiocytes
C
miRNAs
Fold Change (log10)
10000
1000
100
10
1
miR839
miR780.2
miR780.1
miR157
miR172
miR166
miR860
Leaves
Meiocytes

Figure 2.

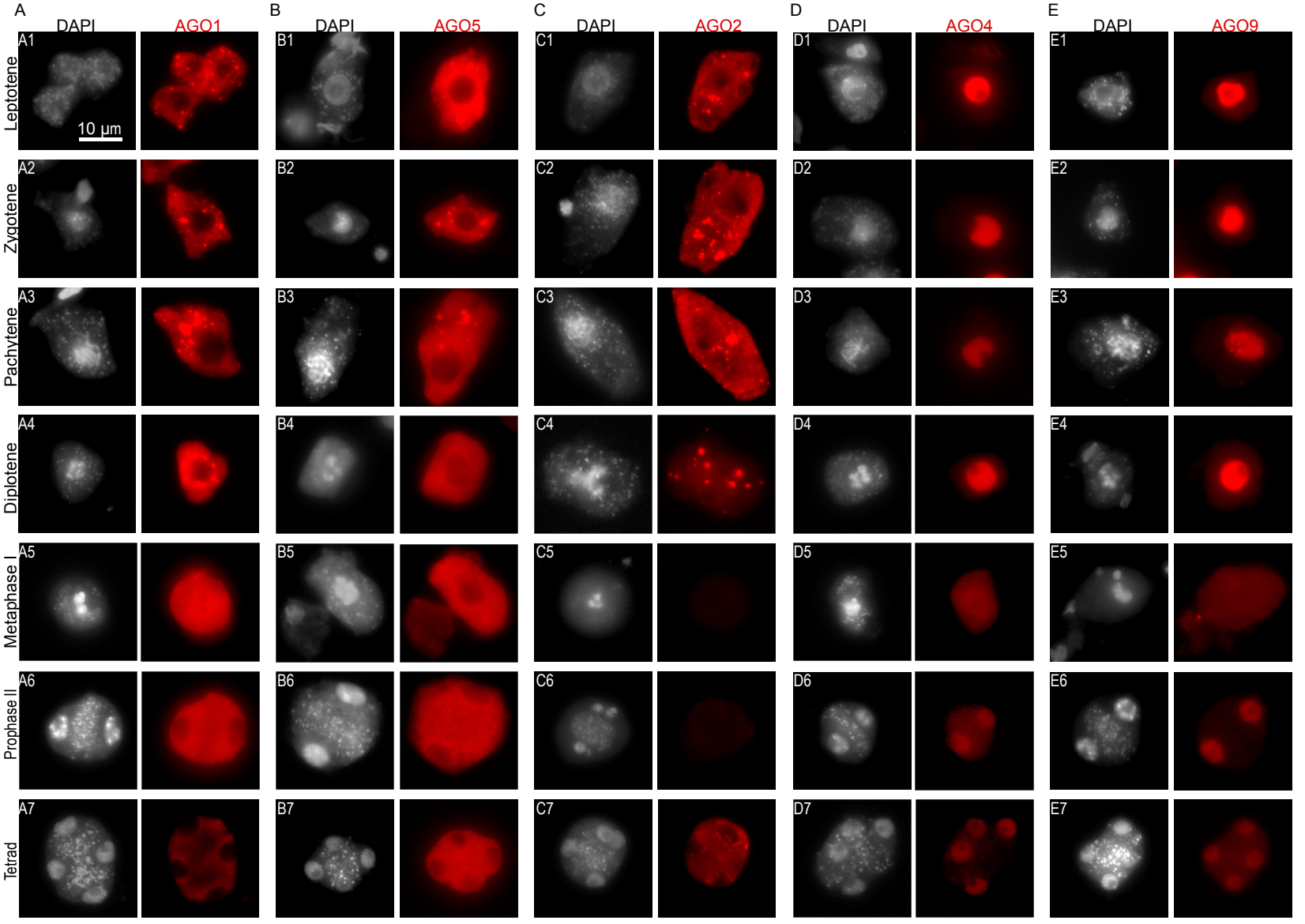
A
DAPI
AGO1
B
DAPI
AGO5
C
DAPI
AGO2
D
DAPI
AGO4
E
DAPI
AGO9
Leptotene
Zygotene
Pachytene
Diplotene
Metaphase I
Prophase II
Tetrad
A1
A2
A3
A4
A5
A6
A7
B1
B2
B3
B4
B5
B6
B7
C1
C2
C3
C4
C5
C6
C7
D1
D2
D3
D4
D5
D6
D7
E1
E2
E3
E4
E5
E6
E7
10 µm